

# Design of Solids for Antigravity Motion Illusion

メタデータ	言語: eng 出版者: Elsevier 公開日: 2019-01-31 キーワード (Ja): キーワード (En): 作成者: 杉原, 厚吉 メールアドレス: 所属:
URL	<a href="http://hdl.handle.net/10291/19881">http://hdl.handle.net/10291/19881</a>

# Design of Solids for Antigravity Motion Illusion

Kokichi Sugihara\*

Meiji University, 4-21-1 Nakano, Nakano-ku, Tokyo 164-8525, Japan

## Abstract

This paper presents a method for designing solid shapes containing slopes where orientation appears opposite to the actual orientation when observed from a unique vantage viewpoint. The resulting solids generate a new type of visual illusion, which we call “impossible motion”, in which balls placed on the slopes appear to roll uphill thereby defying the law of gravity. This is possible because a single retinal image lacks depth information and human visual perception tries to interpret images as the most familiar shape even though there are infinitely many possible interpretations. We specify the set of all possible solids represented by a single picture as the solution set of a system of equations and inequalities, and then relax the constraints in such a way that the antigravity slopes can be reconstructed. We present this design procedure with examples.

**Keywords:** Visual illusion, antigravity slope, picture interpretation, impossible motion

## 1 Introduction

This paper presents a computational approach to design a new visual illusion. Visual illusion is a perceptual behavior where what we “see” differs from the physical reality. This phenomenon is important in vision science because it helps us to understand the nature of human perception [7, 8]. Numerous traditional visual illusions are known, most of which are generated by two-dimensional pictures and their motions [5, 15].

However, very few visual illusions are known that make use of three-dimensional solid shapes. An early example was the Ames room, where a person looks taller when he moves from one corner of the room to another [3]. Other examples include impossible solids produced by a hidden-gap trick [1], and those without hidden gaps [13]. The latter class was extended to include a new type of illusion called “impossible motion” [14].

The design of illusions using solids requires mathematics, because this process can be counterintuitive.

---

\*This manuscript was published in *Computational Geometry: Theory and Applications*, vol. 47 (2014), pp. 675–682.

This paper concentrates on one class of such solids called “antigravity slopes”, in which balls appear to roll uphill against the law of gravity and produce appearances of an “impossible motion”.

In Section 2, we briefly review picture interpretation theory, which specifies the set of all possible solids represented by a picture, and in Section 3 we show that antigravity slopes cannot be constructed using that formulation. In Section 4, we remove some of the constraints by changing structures in the hidden part so that design of antigravity slopes becomes possible. We show some examples in Section 5, and provide concluding remarks in Section 6.

## 2 Reconstruction of a Solid from a Picture

Our goal is to construct solids that generate a visual illusion. As a tool to achieve this goal, let us review picture interpretation theory, by which we can specify all solids represented by a given picture.

For two points  $p$  and  $q$ , let  $\overline{pq}$  denote the closed line segment connecting  $p$  and  $q$ . Let  $(p_1, p_2, \dots, p_n)$  be a sequence of mutually distinct points in two-dimensional space. We assume that the line segments  $\overline{p_1p_2}, \overline{p_2p_3}, \dots, \overline{p_{n-1}p_n}$  and  $\overline{p_np_1}$  do not intersect except at their terminal points. Then, the region bounded by the cyclic sequence of these line segments is called a *polygon* (not necessarily convex). The points  $p_1, p_2, \dots, p_n$  are called *vertices* and the line segments  $\overline{p_1p_2}, \overline{p_2p_3}, \dots, \overline{p_{n-1}p_n}$  and  $\overline{p_np_1}$  are called *edges* of the polygon. Intuitively a polygon is a piece of hard thin flat plate whose boundary is composed of line segments. We place a finite number of polygons in three space, and thus construct a solid object. Formally we define a *solid object* as a collection of a finite number of polygons placed in three space. A solid object is also called a *solid* for short. The polygons that constitute a solid are called *faces*.

For example, the solid  $P$  in Fig. 1 is a hexahedron. This object can be considered a solid composed of the six boundary faces; we do not care whether the inside is occupied with material or empty.

Our goal is to construct an antigravity slope, which is a solid object typically composed of a base plate, slopes, and supporting columns. A slope is composed of a slide and two side walls; they can all be considered as polygons. A support column is a polyhedron, but we consider it as a collection of surface polygons. As shown in Fig. 1, let  $P$  be a solid object fixed to three space with the  $(x, y, z)$  Cartesian coordinate system, and  $D$  be its projection on the plane  $z = 1$  with respect to the center of projection at the origin  $O$ . This means that we see the object from the viewpoint at the origin, and get its image on the plane  $z = 1$ . We assume that all the edges of  $P$  are drawn in  $D$ , and hence  $D$  is called the *line drawing* of  $P$ . Let  $f$  be a face of a solid. We denote by  $[f]$  the image of  $f$  projected on the plane  $z = 1$ . Similarly for a vertex  $v$  of a solid, we denote by  $[v]$  the image of  $v$  on the plane  $z = 1$ .

If  $P$  is given,  $D$  is uniquely determined. On the other hand, if  $D$  is given, an associated  $P$  is not unique in general. If  $D$  represents a solid object correctly, there are infinitely many solids that generate  $D$ . If  $D$  is incorrect in the sense

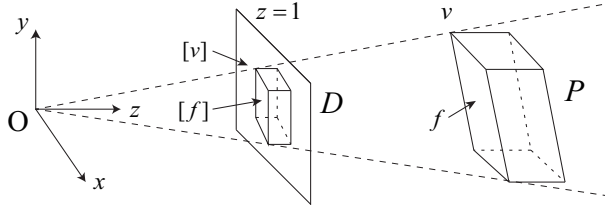


Figure 1: Solid and its central projection.

that it does not represent a solid object, there is no corresponding  $P$ . So we consider how to specify the set of all solid objects that can generate  $D$ .

Suppose that we are provided  $D$  and the relative relations among the vertices and the faces of the solid object. Let  $V = \{v_1, v_2, \dots, v_n\}$  and  $F = \{f_1, f_2, \dots, f_m\}$  be the set of vertices and of faces, respectively, of a solid in three space. Let  $\text{ON}(v_i, f_j)$  represent the predicate stating that the vertex  $v_i$  is on the face  $f_j$ . Similarly let  $\text{NEARER}(v_i, f_j)$  represent “ $v_i$  is nearer than the plane containing  $f_j$ ”, and  $\text{FARTHER}(v_i, f_j)$  represent “ $v_i$  is farther than the plane containing  $f_j$ ”, where “near” and “far” are meant according to the distance from the viewpoint at the origin to each part of the object.

For example, consider the line drawing in Fig. 2. Let us concentrate on the three vertices  $v_i, v_j, v_k$  and face  $f_\ell$  in this figure. Since vertex  $v_i$  is on face  $f_\ell$ , we get

$$\text{ON}(v_i, f_\ell).$$

The edge labeled + in Fig. 2 represents a ridge of a mountain, and hence, if we extend the plane  $f_\ell$ , it passes between the viewpoint and the vertex  $v_j$ . Hence we get

$$\text{FARTHER}(v_j, f_\ell).$$

The edge labeled –, on the other hand, forms the bottom of a valley, and hence the face  $f_\ell$  when extended goes beyond  $v_k$ . Hence we get

$$\text{NEARER}(v_k, f_\ell).$$

We assume that, in addition to the line drawing, we are provided all those predicates satisfied by the solid and we are interested in judging the reconstructability of a solid from the line drawing.

For the  $i$ -th vertex  $v_i$  of the solid, let  $(x_i, y_i, 1)$  be the coordinates of the image  $[v_i]$  of  $v_i$ . Because the original vertex  $v_i$  should be on the ray emanating from the origin and passing through the image  $[v_i]$ , we can express the coordinates of the original vertex in space as  $(x_i/t_i, y_i/t_i, 1/t_i)$ , where  $t_i$  is an unknown parameter representing the inverse of the depth of the vertex from the viewpoint measured along the  $z$  axis.

Let

$$a_j x + b_j y + c_j z + 1 = 0 \tag{1}$$

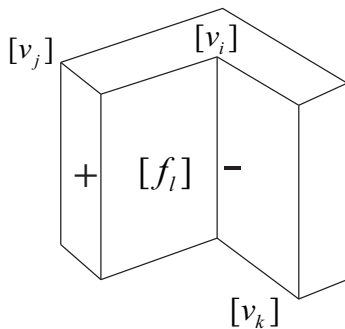


Figure 2: ON, NEARER and FARTHER predicates between faces and vertices.

be the plane containing the  $j$ -th face  $f_j$ , where  $a_j, b_j$  and  $c_j$  are all unknown.

Suppose that  $\text{ON}(v_i, f_j)$  is true. Then, we can substitute the coordinates of  $v_i$  into the equation of  $f_j$ , and thus we get

$$a_j x_i + b_j y_i + c_j + t_i = 0, \quad (2)$$

which is linear in the unknowns  $t_i, a_j, b_j$  and  $c_j$ . Similarly, if  $\text{NEARER}(v_i, f_j)$  is true, we get

$$a_j x_i + b_j y_i + c_j + t_i < 0, \quad (3)$$

and if  $\text{FARTHER}(v_i, f_j)$  is true, we get

$$a_j x_i + b_j y_i + c_j + t_i > 0. \quad (4)$$

We collect all equations of the form (2), one for each ON predicate, and denote the resulting system of equations as

$$Aw = 0, \quad (5)$$

where  $w = (t_1, \dots, t_n, a_1, b_1, c_1, \dots, a_m, b_m, c_m)^t$  is the vector of unknown variables ( $t$  represents the transpose) and  $A$  is a constant matrix. Similarly, we collect all inequalities of the form (3) and (4), and denote the resulting system of inequalities as

$$Bw > 0, \quad (6)$$

where  $B$  is a constant matrix, and the inequality symbol “ $>$ ” represents componentwise inequality.

We can prove that the picture represents a three-dimensional solid if and only if the system consisting of (5) and (6) has a solution [10, 12].

When we, human beings, see a line drawing of an ordinary solid, such as the one in Fig. 2, we are apt to interpret it as a unique solid up to scaling. However, there is usually freedom in interpretations, because any solution of the system of (5) and (6) corresponds to a solid represented by the line drawing. This gap

between human perception and the solutions of (5) and (6) can be utilized to mislead human perception.

For example, the picture in Fig. 3 belongs to a class called *pictures of impossible objects*, because the solid structure we perceive most naturally from the picture seems unrealizable. This picture, in particular, is called an “endless loop of stairs”, which was presented by Penrose and Penrose [6] and is famous because it was used by Dutch artist M. C. Escher in his artwork “Ascending and Decending” (1960).

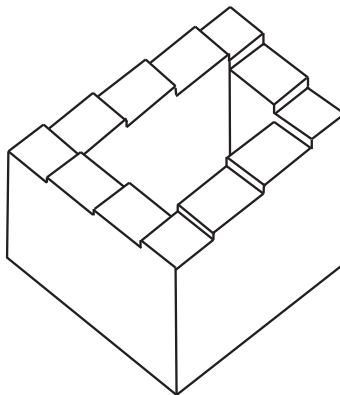


Figure 3: Picture of an impossible object “Endless loop of stairs”.

Although it is called an impossible object, it is not impossible. We can construct a solid structure as shown in Fig. 4, where (a) shows the solid seen from the same viewpoint as the line drawing, and (b) shows the same solid seen from another angle.

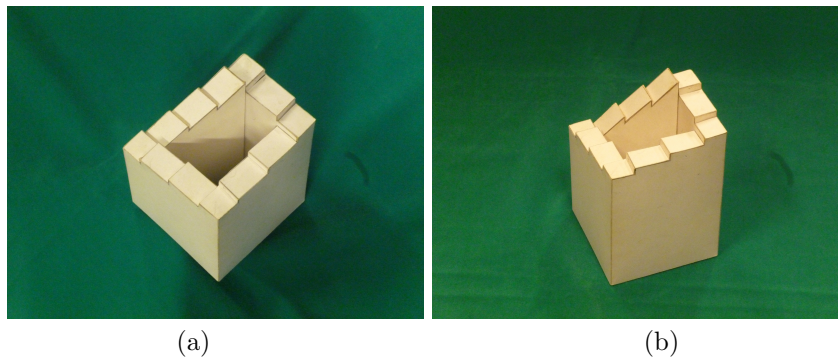


Figure 4: Three-dimensional realization of the impossible object in Fig. 3.

This solid was found in the following manner. We first list all faces and vertices drawn in Fig. 3, next gave ON, NEARER and FARTHER predicates, and finally constructed the associated system of (5) and (6). This system admits

many solutions, and hence we can choose any one of them, obtaining a solid such as the one shown in Fig. 4.

This way, the system of (5) and (6) helps us to construct actual solids that look impossible. Many other examples of such “impossible objects” can be found in [13].

**Remark 1.**

It has been known that the endless loop of stairs can be constructed if we use discontinuous structure, which looks connected when we see it from a special vantage viewpoint. An example of such a structure can be seen in the movie “Inception” (2010) [16, 17].

Note that, on the other hand, the discontinuity trick is not used in the object in Fig. 4. Because we place ON predicates for all pairs of vertices and faces that look incident to each other, the resulting solid is continuous. In this sense, the solid in Fig. 4 is different from a well known realization.

**Remark 2.**

The system of (5) and (6) is sometimes unrobust for judging the realizability of a solid object from a line drawing, because numerical errors in vertex locations in the picture plane, even if they are very small, may generate inconsistency in (5) and (6). This situation can be understood if we consider a hexahedron. Let  $P$  be a hexahedron and  $D$  be its image. Since  $P$  has eight vertices and six faces, there are  $8 + 3 \times 6 = 26$  unknown variables  $t_1, t_2, \dots, t_8, a_1, b_1, c_1, \dots, a_6, b_6, c_6$ . On the other hand, since each of the six faces has four vertices, the system (5) has  $6 \times 4 = 24$  equations. Thus, the system (5) consists of 24 equations with respect to 26 unknown variables. This means that the system (5) is redundant, because the difference between the number of variables and that of equations is 2, although there should be at least 4 degrees of freedom (i.e., three degrees of freedom in the choice of one face and one more degree in the choice of the thickness of the hexahedron) in the system (5) if the picture  $D$  correctly represents a hexahedron. This property in turn implies that if the vertex locations in the picture plane contain errors, the rank of the matrix  $A$  changes and the system becomes unsatisfiable even though the picture looks correct to human eyes.

This unrobustness can be overcome by removing redundant equations from the system (5); this can be done efficiently by employing network flow algorithms. Refer to [4, 11] for details.

### 3 Impossibility of Antigravity Slopes

The system of (5) and (6) is a powerful tool for realizing three-dimensional solids from impossible pictures, but is not all-powerful. Indeed for many impossible pictures, the system of (5) and (6) does not admit solutions at all, and hence we cannot realize three-dimensional structures.

As a typical class of such impossible structures, we concentrate on antigravity slopes. Let us consider the picture of a simple solid in Fig. 5, in which a slope is supported by two columns standing on a base plate. The broken lines represent

the hidden parts. However, to avoid unnecessary complexity, some hidden parts are omitted.

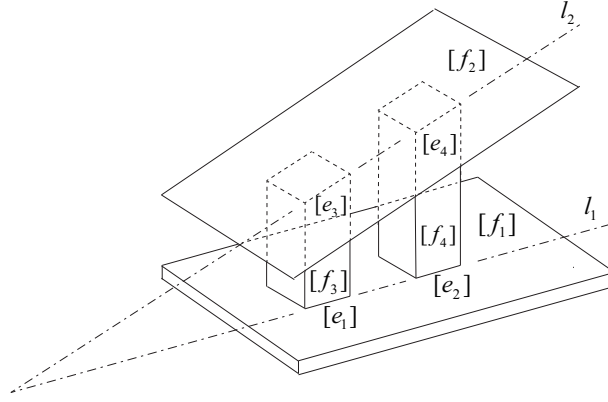


Figure 5: Slope supported by two columns.

The solid object shown in Fig. 5 is the most fundamental structure of the antigravity slope. Actually we can use this structure as a gadget to construct more complicated antigravity slopes by combining two or more copies of this gadget. So we concentrate on this structure and see how we can convert a normal slope into an antigravity slope.

Let  $f_1$  denote the top face of the base plate, and  $f_2$  denote the slope plane. Assume that, for each of the two columns, all four lower vertices are on  $f_1$  and are farther than  $f_2$ , while all four upper vertices are on  $f_2$  and are nearer than  $f_1$ . We also assume that  $f_1$  is horizontal. Then, we usually expect that the slope  $f_2$  tilts to the left, that is, the right end of  $f_2$  is higher than the left end. Indeed, the system of equations (5) and inequalities (6) accepts such a slope as its solution.

Now we ask whether the set of solutions contains a slope that tilts to the right? The answer is “no”. In every solid whose projection matches that of the picture shown in Fig. 5, the slope  $f_2$  tilts to the left. This can be understood in the following way. As shown in Fig. 5, let  $f_3$  and  $f_4$  be the right front faces of the left and right columns,  $e_1$  and  $e_2$  be the lower edges of  $f_3$  and  $f_4$ , and  $e_3$  and  $e_4$  be the upper edges of  $f_3$  and  $f_4$ , respectively. Because the edge images  $[e_1]$  and  $[e_2]$  are collinear in the picture plane, and the corresponding original edges  $e_1$  and  $e_2$  are on  $f_1$ ,  $e_1$  and  $e_2$  must also be collinear in three space. Let  $l_1$  be a line in space containing  $e_1$  and  $e_2$ . Similarly, because  $[e_3]$  and  $[e_4]$  are collinear in the picture plane and the corresponding spatial edges  $e_3$  and  $e_4$  are on  $f_2$ , they are collinear in three space. Let  $l_2$  be the line containing  $e_3$  and  $e_4$ . Note that  $e_1$  and  $e_3$  are coplanar because they are on  $f_3$ ; thus  $l_1$  and  $l_2$  are coplanar, which implies that  $f_3$  and  $f_4$  are coplanar. Because  $l_1$  and  $l_2$  meet to the left of the solid, the slope  $f_1$  tilts to the left.

This property holds for any solution of the system of (5) and (6) associated

with the picture shown in Fig. 5. Therefore, it is impossible to construct a slope that tilts to the right from the picture shown in Fig. 5. Therefore, in order to realize three-dimensional structures that mislead human perception, we need some additional technique for this class of “impossible structures”. We will develop it in the next section.

## 4 Construction of an Antigravity Slope

Our goal is to construct a slope that tilts to the right, but such a slope is not contained in the solutions of (5) and (6). Thus we want to construct a solid such that the visible part is exactly the same as that of Fig. 5, all the incidence relations between the vertices and the faces are also the same, but the slope tilts to the right. To achieve this, we can modify the picture around the upper parts of the two columns because they are hidden by the slope. The vertices at the top of the columns can be moved slightly along the associated vertical edges of the columns. Here “slightly” means that the movements of the vertices are restricted to the area covered by  $[f_2]$  in the picture plane.

For this purpose we first show one natural formulation. However, this leads to a nonlinear system which is not easy to solve. Therefore, we next switch the formulation to another, which is rough but remains linear, and hence can be used to achieve our goal.

As shown in Fig. 6, let  $e_i, i = 5, 6, \dots, 12$ , be the eight vertical edges of the left and right columns, and let  $v_i$  be the top vertices incident to  $e_i$ . Let  $(\alpha_i, \beta_i, 0)$  be the unit vector parallel to the image  $[e_i]$  in the picture plane. Note that  $\alpha_i = 0$  does not necessarily hold; the images of the column edges are not necessarily vertical in a strict sense, because the picture is the perspective projection of a solid. We replace the coordinates  $(x_i, y_i, 1)$  of the vertex  $[v_i]$  with

$$(x_i + s_i\alpha_i, y_i + s_i\beta_i, 1), \quad i = 5, 6, \dots, 12 \quad (7)$$

where  $s_i$  is a new unknown parameter. This change of the coordinates of vertex  $[v_i]$  implies that we move the vertex along the line containing the edge  $e_i$ . Because  $v_i$  is hidden by the face  $f_2$ , slight movement of  $v_i$  does not change the visible part of the edge  $e_i$ . Then, instead of the equation (2), the predicate  $\text{ON}(v_i, f_i)$  is represented by

$$a_i(x_i + s_i\alpha_i) + b_i(y_i + s_i\beta_i) + c_i + t_i = 0. \quad (8)$$

The inequalities of the form (3) and (4) are also changed by replacing  $x_i$  and  $y_i$  with  $x_i + s_i\alpha_i$  and  $y_i + s_i\beta_i$ , respectively. Let us change the equations and inequalities associated with all the upper vertices of the columns, and denote the resulting equations and inequalities by

$$\bar{A}(s)w = 0, \quad (9)$$

$$\bar{B}(s)w > 0, \quad (10)$$

where  $s = (s_5, s_6, \dots, s_{12})$  is the vector of unknown parameters introduced by the movement of the hidden vertices, and  $\bar{A}(s)$  and  $\bar{B}(s)$  are the resulting coefficient matrices corresponding to the equations (5) and the inequalities (6).

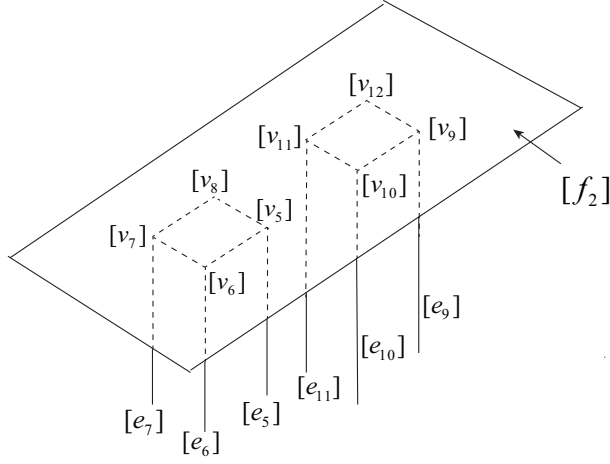


Figure 6: Upper part of the fundamental slope.

The new system of equations (9) and inequalities (10) allows a solution corresponding to a slope tilting to the right, that is, an antigravity slope.

However, (9) and (10) are nonlinear because the matrices  $\bar{A}(s)$  and  $\bar{B}(s)$  contain unknown variables. Hence, unlike for the system of (5) and (6), it is not straightforward to specify the set of all solutions. To circumvent this difficulty, we change our strategy. In what follows instead of introducing new variables  $s_5, s_6, \dots, s_{12}$ , we temporarily ignore some of the ON predicates and thus increase the degree of freedom of the equations. Note that we have

$$\text{ON}(v_i, f_2), \quad i = 5, 6, \dots, 12 \quad (11)$$

in the original solid structure. Among them we adopt two predicates

$$\text{ON}(v_5, f_2) \quad \text{and} \quad \text{ON}(v_9, f_2) \quad (12)$$

but delete the other six predicates

$$\text{ON}(v_i, f_2), \quad i = 6, 7, 8, 10, 11, 12, \quad (13)$$

and reconstruct the linear equations (5) and the inequalities (6). Because we remove the six constraints in (13), the two edges  $e_5$  and  $e_9$  are not necessarily parallel and hence the two columns can slant in different angles. Therefore it is possible that the left column stands almost vertical while the right column slants much so that the vertex  $v_5$  is higher than the vertex  $v_9$  in three space. Thus, the system has a solution corresponding to slopes tilting to the right, and

so we choose one of them. In this solid, the six vertices  $v_6, v_7, v_8, v_{10}, v_{11}, v_{12}$  are not necessarily on  $f_2$ , because the associated equations were deleted. So next we find the points of intersection between the slope and the edges  $e_i, i = 6, 7, 8, 10, 11, 12$ . Let the points of intersection be  $v'_i, i = 6, 7, 8, 10, 11, 12$ . We move the vertices  $v_i$  to the associated point of intersection  $v'_i$ . Thus we obtain a solid in which all their original incidence predicates are satisfied. In this solid, some of the vertices are moved from the original positions. However, if the movement of the vertices is restricted in the slope polygon, they are all hidden. Therefore, the visible part of the solid is the same as represented by the original picture. This is our idea for constructing antigravity slopes.

Assume that all vertices at the top of the columns are strictly inside the slope polygon in the picture plane. In other words, assume that none of  $[v_i], i = 5, 6, \dots, 12$  in Fig 6 are on the boundary of the image  $[f_2]$ . Then, we can always find a slope in which  $[v_i], i = 5, 6, \dots, 12$  are all inside  $[f_2]$ . This is because if the slope polygon  $f_2$  moves close to the top face  $f_1$  of the base plate, the images  $[v'_i]$  of the points of intersection converge to the original locations  $[v_i]$  for  $i = 5, 6, \dots, 12$ .

This procedure can be summarized in the following algorithm.

**Algorithm 1** (most fundamental antigravity slope)

Input: A picture  $D$  of a slope supported by two columns, called the longer column and the shorter column standing vertically on a base plate.

Output: A solid whose visible part coincides with the visible part of  $D$  and whose slope descends from the shorter column to the longer column.

Procedure:

1. Remove the ON predicates between the slope and three of the four vertices on the top of each of the two columns.
2. Construct the system of equations (5) and inequalities (6) for the resulting solid object.
3. Choose a solution of (5) and (6) that corresponds to a slope plane that tilts from the shorter column to the longer column. (A practical procedure to achieve this step will be described immediately after this algorithm.)
4. Recover the ON predicates removed in Step 1 by finding the points of intersection between the slope and the associated edges.
5. If the points of intersection found in Step 5 are inside the slope polygon, report the resulting solid object as the output. Otherwise go to Step 3 and choose another solution of (5) and (6) such that the slope is more gentle.  $\square$

Step 3 of Algorithm 1 can be achieved in the following way. Recall that the solutions of the system of equations (5) have at least four degrees of freedom. Indeed, we can choose the three-dimensional position of a plane containing an arbitrarily chosen face and one more vertex outside this face to fix a solution (i.e., a solid). Therefore, Step 3 can be achieved first by specifying the orientation of the slope  $f_2$  by choosing the values of variables  $a_2, b_2$  and  $c_2$ , and next by specifying some of other variables until a solution is fixed uniquely. Thus we can choose the orientation of the slope as we want.

## 5 Examples

We can use the fundamental solid constructed by Algorithm 1 as a gadget to construct more complicated antigravity slopes. Figs. 7, 8 and 9 show examples of antigravity slopes. In each of them, (a) shows a solid that looks the same as represented by the original picture, and hence the orientation of the slopes are perceived opposite to the actual orientation, (b) shows the same solid seen from another angle.

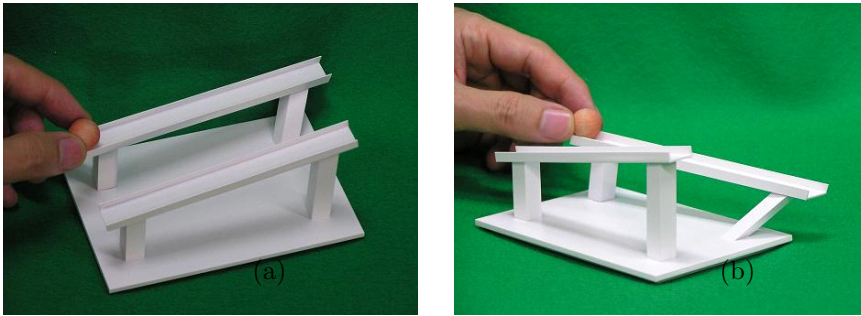


Figure 7: “Antigravity Parallel Slopes”.

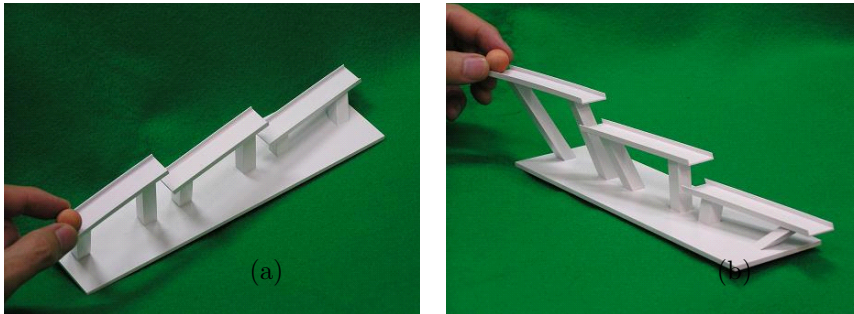


Figure 8: “Antigravity Cascade of Three Slopes”.

They generate impossible motions in the sense that when we place balls on the slopes, they look like they are rolling uphill on the slope against the gravity law.

The solid in Fig. 7 looks like two parallel slopes both tilting to the left, but the fact is that the nearer slope actually tilts to the left as it appears to be, while the farther slope tilts to the right against its appearance. Thus, this solid is composed of one normal slope and one antigravity-slope gadget. So, if we put a ball on the nearer slopes, it rolls downhill as expected, but if we put a ball

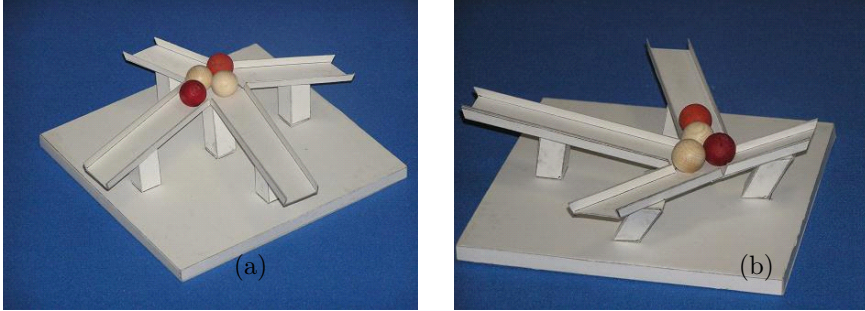


Figure 9: “Magnet-Like Slopes”.

on the other slope, it rolls uphill against our expectation; thus an illusion of an impossible motion is created.

The solid in Fig. 8 looks like three parallel slopes cascaded one after another; all tilting to the left. However, if we put a ball on the leftmost slope, it rolls uphill to the right end, jumps on the second slope, rolls uphill, jumps on the rightmost slope, and finally rolls uphill, falling down at the right end of the slope. As shown in fig. 8(b), this solid is composed of three antigravity-slope gadgets.

The solid in Fig. 9 looks like four slopes tilting in four directions from the highest center. However, if we put balls on any slopes, they look rolling uphill toward the highest center; thus impossible motion is created. The fact is that the center is the lowest and all four slopes tilts toward the center. This solid is composed of four antigravity-slope gadgets connected at the central plate. The antigravity motion illusion generated by this solid got the first prize in the Best Illusion of the Year Contest 2010 held at Florida in May 2010. We can enjoy this impossible motion on the web page [18].

## 6 Concluding Remarks

We have presented our basic idea for constructing antigravity slopes. When we see those slopes from a special viewpoint, the orientations of the slopes look opposite to the actual orientations, and hence they generate the visual illusion of an impossible motion of rolling balls. This is a new computational approach to visual illusion.

Remaining tasks for future work/research include the increase of variants of antigravity slopes, the extension to other types of impossible motions, and the extension to curved-face solids. We also want to study human visual perception through visual illusion of impossible motions. They are future problems in basic research.

As for applications of antigravity slopes, we want to develop methods for decreasing the strength of the illusion. It is known that one of the reasons

of natural congestion of traffic flow in a highway is drivers' misperception of slope orientations [2]. If we understand the human illusion mechanism in slope perception, we would suggest the shape of new highways in which the true orientations of the slopes can be easily perceived. We would also suggest possible ways of arranging the environment of existing highways so that the slope illusion is not evoked.

## Acknowledgments

This work is partially supported by the Grant-in-Aid for Scientific Research (B) No. 20360044 of MEXT.

## References

- [1] B. Ernst: *The Eye Beguiled: Optical Illusion*. Benedikt Taschen, 1986.
- [2] S. Goto and H. Tanaka (eds.): *Handbook of Visual Illusion Science* (in Japanese). University of Tokyo Press, Tokyo, 2005.
- [3] R. L. Gregory: *The Intelligent Eye*. Weidenfeld & Nicolson, London, 1970.
- [4] H. Imai: On combinatorial structures of line drawings of polyhedra. *Discrete Applied Mathematics*, Vol. 10 (1985), pp. 79–92.
- [5] J. Ninio: *The Science of Illusions*. Comstock Pub. Assoc., New York, 2001.
- [6] L. S. Penrose and R. Penrose: Impossible objects: A special type of visual illusion. *British Journal of Psychology*, Vol. 49 (1958), pp. 31–33.
- [7] J. O. Robinson: *The Psychology of Visual Illusion*. Dover Publications, New York, 1998.
- [8] A. Seckel: *Optical Illusions: The Science of Visual Perception*. Firefly Books Ltd., New York, 2009.
- [9] K. Sugihara: Mathematical structure of line drawings of polyhedrons—Toward man-machine communication by means of line drawings. *IEEE Transactions on Pattern Analysis and Machine Intelligence*, Vol. PAMI-4 (1982), pp. 458–469.
- [10] K. Sugihara: A necessary and sufficient condition for a picture to represent a polyhedral space. *IEEE Transactions on Pattern Analysis and Machine Intelligence*, Vol. PAMI-6 (1984), pp. 578–586.
- [11] K. Sugihara: Detection of structural inconsistency in systems of equations with degrees of freedom and its applications. *Discrete Applied Mathematics*, Vol. 10 (1985), pp. 297–312.
- [12] K. Sugihara: *Machine Interpretation of Line Drawings*. MIT Press, 1986.

- [13] K. Sugihara: Three-dimensional realization of anomalous pictures — An application of picture interpretation theory to toy design. *Pattern Recognition*, Vol. 30 (1997), pp. 1061–1067.
- [14] K. Sugihara: A characterization of a class of anomalous solids. *Interdisciplinary Information Sciences*, Vol. 11 (2005), pp. 149–156.
- [15] J. Timothy Unruh: *Impossible Objects: Amazing Optical Illusions to Confound and Astound*. Sterling Publishing Co., Inc., New York, 2001.
- [16] <http://www.youtube.com/watch?v=uUzBIR-dOwg>
- [17] <http://www.youtube.com/watch?v=-B7ifky4QQU>
- [18] <http://www.youtube.com/watch?v=hAXm0dIuyug>